Solar Physics (2005) 232: 87–103

MULTIPLE TYPE II SOLAR RADIO BURSTS

A. SHANMUGARAJU
Department of Physics, Arul Anandar College, Karumathur 625514, Madurai, India; Korea Astronomy and Space Science Institute (KASI), Whaamdong, Yuseong-gu, Daejeon 305-348, Korea

Y.-J. MOON, K.-S. CHO and Y.-H. KIM
Korea Astronomy and Space Science Institute (KASI), Whaamdong, Yuseong-gu, Daejeon 305-348, Korea
(e-mail: yjmoon@kasi.re.kr)

M. DRYER
NOAA Space Environment Center, Boulder, Colorado 80305, U.S.A.
(e-mail: murray.dryer@noaa.gov)

and

S. UMAPATHY
School of Physics, Madurai Kamaraj University, Madurai, India

(Received 1 May 2005; accepted 11 July 2005)

Abstract. We report on the detailed analysis of a set of 38 multiple type II radio bursts observed by Culgoora radio spectrograph from January 1997 to July 2003. These events were selected on the basis of the following criteria: (i) more than one type II were reported within 30 min interval, (ii) both fundamental and harmonic were identified for each of them. The X-ray flares and CMEs associated with these events are identified using GOES, Yohkoh SXT, SOHO/EIT, and SOHO/LASCO data. From the analysis of these events, the following physical characteristics are obtained: (i) In many cases, two type IIs with fundamental and harmonic were reported, and the time interval between the two type IIs is within 15 min; (ii) The mean values of starting frequency, drift rate, and shock speed of the first type II are significantly higher than those of the second type II; (iii) More than 90% of the events are associated with both X-ray flares and CMEs; (iv) Nearly 75% of the flares are stronger than M1 X-ray class and 50% of CMEs have their widths larger than 200° or they are halo CMEs; (v) While most of the first type IIs started within the flare impulsive phase, 22 out of 38 second type IIs started after the flare impulsive phase. Weak correlations are found between the starting and ending frequencies of these type II events. On the other hand, there was no correlation between two shock speeds between the first and the second type II. Since most of the events are associated with both the flares and CMEs, and there are no events which are only associated with multiple impulsive flares or multiple mass ejections, we suggest that the flares and CMEs (front or flank) both be sources of multiple type IIs. Other possibilities on the origin of multiple type IIs are also discussed.

1. Introduction

The magnetohydrodynamic (MHD) shocks generated by flares and/or coronal mass ejections (CMEs) are observed as type II radio bursts in the solar corona (cf. Nelson and Melrose, 1985). Most of the type IIs have fundamental and harmonic signatures in the dynamic spectrum. As reported by Robinson and Sheriden (1982), and Gergely *et al.* (1984), a multiple type II burst consists of multiple bands in the dynamic spectrum. These bands often have different frequency drift rates or are significantly displaced in frequency in a manner different from the normal fundamental–harmonic or split-band relationships (Nelson and Melrose, 1985; Vrsnak *et al.*, 2001). The presence of these multiple bands may indicate the interaction of a single shock front with different coronal structures. Alternatively, the various bands may indicate successive shocks. Thus, the study of multiple type IIs, shocks and their physical origin is of great interest.

However, the study of multiple type II bursts is rare. For example, Robinson and Sheriden(1982) reported that nearly 20% of all the type IIs are multiple type IIs. From 145 multiple type II events observed during 1968–1981 at Culgoora, a set of 20 clear multiple type II events were selected and their characteristics were studied. They found that most of them were associated with mass ejections and flares. However, the properties of the flares and CMEs were not studied. They concluded that multiple type II events arise from a single shock wave, which interacts with different coronal structures since there were no multiple disturbances. Gergely *et al.* (1984) reported a multiple type II burst associated with a coronal transient on May 8, 1981. This transient was related to an M7.7/2B flare at N10E38 and was associated with at least two coronal type II bursts. They simulated the two shocks with a 2.5D MHD model (Dryer *et al.*, 1979, and references therein). With two assumed pressure pulses, two shocks (1200 and 1500 km/s, respectively, just minutes apart) were formed, presumably from two mimicked flares that originated at two locations within AR3039.

The suggestion of two kinds of coronal shocks was first made by Maxwell and Dryer (1982) and Gergely *et al.* (1984) from an observational and theoretical viewpoint and then by different authors (Robinson and Sheridan, 1982; Robinson, 1985; Kaiser *et al.*, 1998; Klassen *et al.*, 1999; Gopalswamy, 2000) from an observational point of view. In the recent literatures, evidence for more than one coronal shock or more than one coronal shock source has been provided (Reiner *et al.*, 2001; Leblanc *et al.*, 2001; Vrsnak, Magdalenic, and Aurass, 2001; Classen and Aurass, 2002; Mann *et al.*, 2003).

Recently, Shanmugaraju *et al.* (2003a) made a detailed investigation of type II radio bursts from 1999 to 2001 to address a question if there exist two kind of coronal shocks. From the analysis of two classes (flare-associated and flare-CME-associated), they found noticeable differences in several aspects. Specifically, seven double type IIs that occurred in 2000 and reported by Culgoora were only observed in the flare-CME-associated ones. Finally, they suggested the existence of more than one driver of coronal shocks. More samples are required to study multiple type IIs, their physical origin, and their interaction with coronal structures.

In this paper, we present a relatively large sample of multiple type IIs (observed between January 1997 and July 2003 at Culgoora) including the seven events reported by Shanmugaraju *et al.* (2003a). Our main aim is to study the physical properties of the different components of multiple type IIs and to find the relationship between the components. The secondary aim is to examine the properties of flares and CMEs associated with these events. To determine the association among the type II events, CMEs, and flares, we have utilized GOES X-ray, Yohkoh SXT, SOHO/LASCO, and SOHO/EIT data.

In the next section, we describe the data analysis. In Section 3, results are given, which are discussed in Section 4. In Section 5, a summary and conclusions are delivered.

2. Data Analysis

Out of many type IIs reported during the period January 1997 to July 2003 in Solar Geophysical Data by the Culgoora spectrograph, we have collected a sample of 38 multiple type II radio bursts. These events were selected on the basis of the following criteria: (i) more than one report of type IIs were reported within 30 min interval, (ii) both fundamental and harmonic were identified for each of them. According to the temporal and spacial coincidences, the flares and CMEs associated with these events are identified using the GOES X-ray flare catalog[1] and the SOHO/LASCO online CME catalog.[2] The catalog values are utilized for analysis. Also we have utilized the Yohkoh SXT data to identify the flare locations. A clear example of a multiple type II event observed by the Culgoora radio spectrograph is shown in Figure 1. As seen in this figure, there were two type II bursts reported (during 04:33–04:45 and 04:47–05:03 UT) within a short interval of 2 min in the frequency range of 160–30 MHz. Each type II burst has fundamental and harmonic signatures.

Table I gives the details of the 38 events: date of observation is given in the first column; the data corresponding to the type IIs (start time of the first drift and end time of the second drift) are given in columns 2 and 3; X-ray flare information (class, start time, end time, and location) are given in columns 4–8; CME data (first appearance time in LASCO C2, width and position angle (PA) in degrees, and speed in kilometer per second) are given in columns 9–12.

3. Results

3.1. Association with flares and CMEs

There are X-ray flare reports for all the 38 events except two cases (980530 and 990611). These two cases have only very weak X-ray enhancements. It is found that nearly 75% (27/36) of the flares have stronger than M1 X-ray class. Eight flares

[1] ftp://ftp.ngdc.noaa.gov/STP/SOLAR_DATA.
[2] http://cdaw.gsfc.nasa.gov/CME_list.

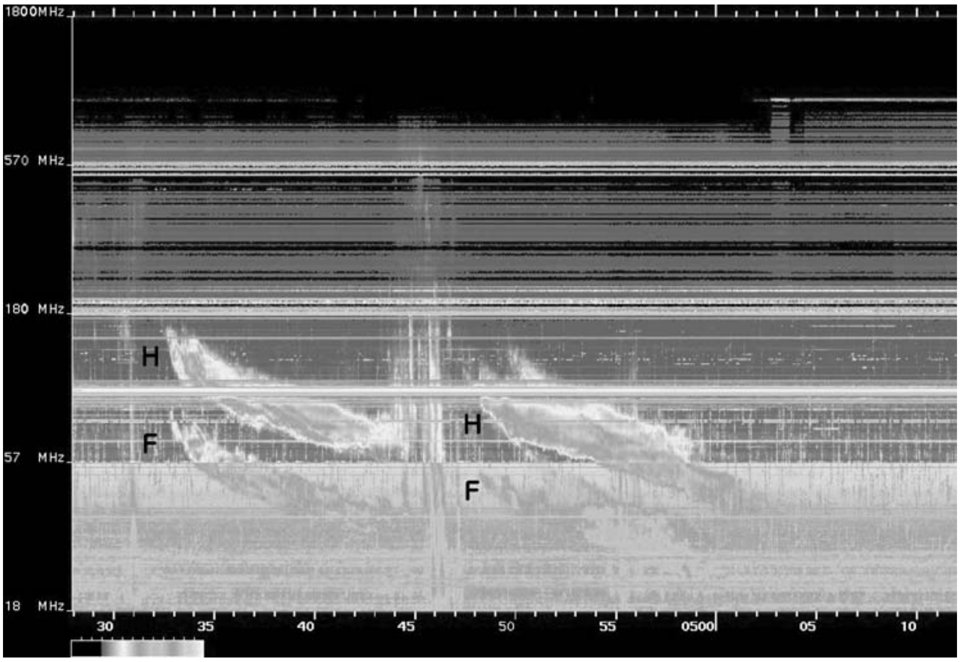

Figure 1. A clear example of a multiple type II event observed by Culgoora on January 23, 2003.

have duration longer than or equal to 45 min. There are CME reports for 30 events (no CME reports for 8 cases, which include SOHO data gaps in 6 cases). Hence, more than 90% (36/38 for flares, and 30/32 for CMEs) of the events are related with flares and CMEs. Out of these, nearly 50% of the CMEs have widths larger than 200° or they are full halo CMEs. In addition, we found an average of the CME speeds around 875 km s^{-1}, which is about two times the CME mean speed and is significantly larger than the mean speed of flare-associated CMEs (Moon *et al.*, 2002). We also examined the correlation between the CME speeds and the type II speeds from the first and the second type II in a multiple type II event. A weak correlation coefficient (0.34) has been found between the reported speeds of type IIs and CMEs (Figure 2a). Reiner *et al.* (2001) found no correlation between metric type II speeds and CME speeds. On the other hand, they found a good correlation (0.71) between decametric–hectametric type II speeds and CME speeds.

Figure 2b shows a very weak correlation (0.27) between X-ray flare importance versus multiple type II speeds. In an analogous graph, a very strong correlation (0.8) was found by Vrsnak (2001), and somewhat lower correlation was obtained by Vrsnak, Magdalenic, and Aurass (2001). The very weak correlation in the present study may be ascribed to the multiple shocks generated by flares and CMEs. However, as seen above and below the best-fit line in Figure 2b, it seems that there exist two different populations.

TABLE I

Multiple type II events and the corresponding X-ray flares and CMEs[a].

	Type II			X-ray flare				CME			
Date	Start	End	Class	Start	Peak	End	Location	Time	PA	Width	Speed
971103	0437	0457	C8.6	0432	0438	0449	S20W13	0528	240	109	227
971104	0558	0617	X2.1	0552	0558	0602	S14W33	0610	Halo	360	785
980125	2135	2238	M1.3	2126	2136	2143	N22E53	2219	89	84	596
980423	0540	0554	X1.2	0535	0555	0623	Limb	0655	308	20	646
980508	0200	0216	M3.1	0149	0204	0217	Limb	0228	286	76	371
980509	0326	0342	M7.7	0304	0340	0355	Limb	0335	262	178	2331
980530	2248	2306	B3.0	–	–	–	Behind	2328	251	63	594
980819	2145	2208	X3.9	2135	2145	2150	N32E75	SOHO	Data	Gap	–
980824	2202	2220	X1.0	2150	2212	2235	N35E09	SOHO	Data	Gap	–
980909	0500	0518	M2.8	0452	0458	0505	Limb	SOHO	Data	Gap	–
980923	0657	0722	M7.1	0640	0713	0731	N18E09	SOHO	Data	Gap	–
981124	0217	0240	X1.0	0207	0220	0237	Limb	0230	Halo	360	1798
981127	0730	0750	M1.6	0721	0743	0757	S24E09	0830	Halo	360	434
981223	0611	0632	M2.3	0513	0659	0743	Behind	SOHO	Data	Gap	–
990403	2307	2345	M4.3	2256	2310	2319	N29E81	2347	74	156	923
990526	0235	0249	C2.3	0225	0230	0235	N22E41	0426	44	71	483
990611	0039	0100	B7.5	–	–	–	Behind	0126	288	101	719
990711	0014	0028	C3.0	0009	0019	0029	N19E36	0131	81	128	318
990802	2129	2158	X1.4	2118	2125	2138	S18W46	2226	271	157	292
991116	0507	0531	M1.8	0447	0512	0545	N18E43	0530	285	129	712
991228	0046	0105	M4.5	0039	0048	0052	N20W56	0054	293	82	672
000212	0403	0419	M1.7	0351	0410	0431	N26W23	0431	Halo	360	1107
000217	2025	2049	M1.3	2017	2035	2107	S29E07	2006	Halo	360	600
000327	0646	0706	C2.3	0637	0654	0714	Behind	0731	129	90	487
001009	2337	2355	C6.7	2319	2343	0021	N01W14	2350	Halo	360	798
001124	0502	0528	X2.0	0455	0502	0508	N23W05	0530	Halo	360	994
001125	0107	0120	M8.2	0059	0131	0201	N07E50	0131	Halo	360	2519
010120	2112	2126	M7.7	2106	2120	2132	S07E46	2130	Halo	360	1507
010520	0604	0624	M6.4	0600	0603	0606	Limb	0626	227	179	546
010611	0554	0609	C7.1	0533	0552	0611	S10W30	0554	–	–	–
011019	0100	0106	X1.6	0047	0105	0113	N16W18	0127	267	254	558
011108	0704	0726	M9.1	0659	0704	0706	S19W19	SOHO	Data	Gap	–
020409	0042	0100	M2.1	0038	0042	0050	N19E46	0127	38	68	310
020412	0458	0509	C3.4	0448	0512	0519	N16E05	0550	–	–	–
021110	0316	0334	M2.4	0304	0321	0335	S12W37	0330	Halo	360	1516
030123	0433	0503	C6.0	0425	0434	0441	S22E21	0530	112	76	234
030423	0101	0115	M5.1	0039	0106	0115	N22W25	0127	271	248	916
030527	2302	2316	X1.3	2256	2307	2313	S07W17	2350	Halo	360	964

[a]If there is a blank, it means there is no report of the corresponding data.

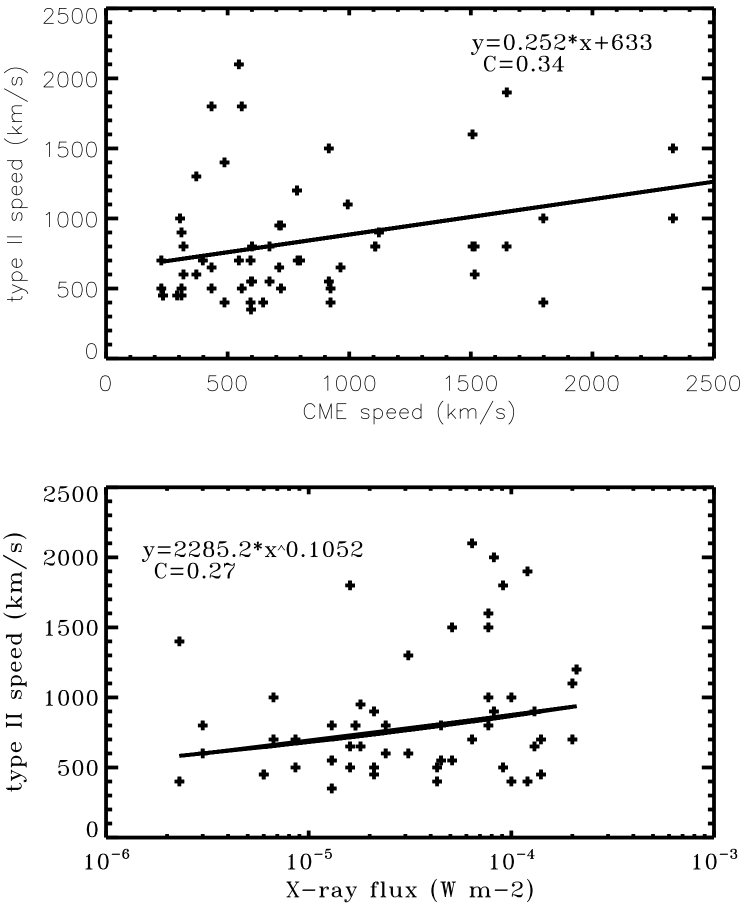

Figure 2. (a) Correlation between CME speed and type II speeds. (b) Correlation between X-ray flare importance and type II speeds.

3.2. Relationship between the two components

For all the events, two type IIs with two different shock speeds are reported except for three cases (980819, 981127, 020409 in which three different shock speeds were reported by Culgoora). We consider the first two type IIs in such an event as two components. The time delay between the start of two components lies between 0 and 20 min (Figure 3). The second component started before the end time of the first component in 16 cases out of 38.

Further, we analyzed the properties of these components. Since the second harmonic is clear in most of the dynamic spectrum, we utilized the data corresponding to the second harmonic. The distributions of the properties (duration, ending frequency, starting frequency, bandwidth, drift rate, shock speed) of the first and second components are shown in Figure 4. On an average, the starting frequency

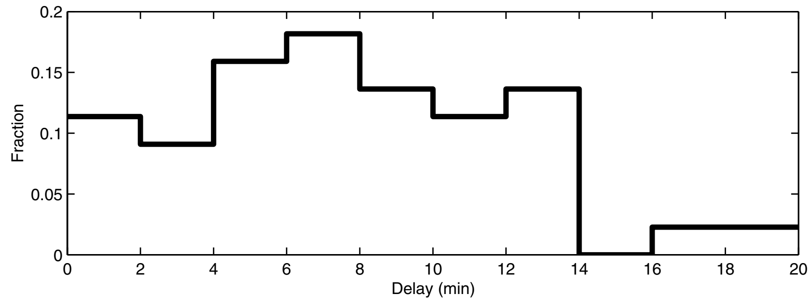

Figure 3. Distribution of the time interval between the two components in multiple type IIs.

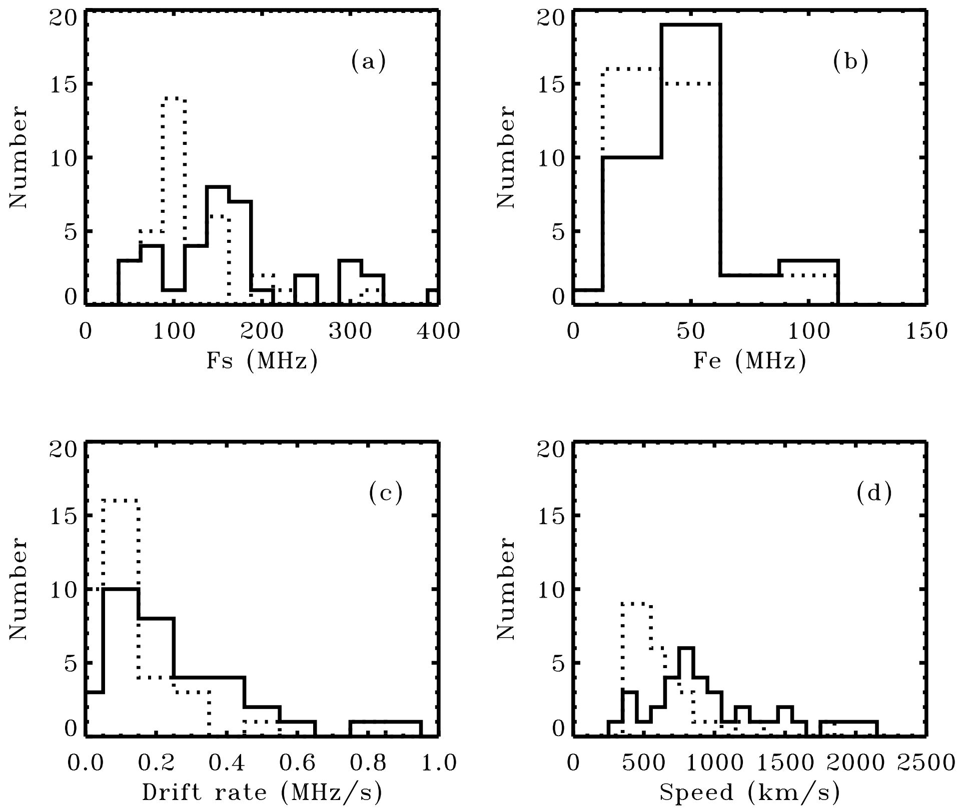

Figure 4. Distributions of the properties (a) starting frequency, Fs; (b) ending frequency, Fe; (c) drift rate; (d) shock speed. Solid line, first component; dashed line, second component.

of the first component seems to be higher than that of the second component. As seen in Figure 4a, a peak lies in the frequency range 150–175 MHz for the first component, whereas it is centered around 100 MHz for the second component. However, the starting frequency of the first component is nearly equal to that of second component in seven cases; and it is less than that of second component in seven other cases. Similar to the distribution of starting frequency, the distributions of ending frequency, drift rate and shock speed of the first component are skewed to the higher values (Figure 4b–d). It is interesting to note that the mean values of starting frequency, drift rate, shock speed (179 MHz, 0.36 MHz s^{-1}, 1008 km s^{-1}) of the first component are significantly higher than those (127 MHz, 0.21 MHz s^{-1}, 657 km s^{-1}) of the second component.

Table II gives the details of the first and second components of 38 multiple type II events: the data corresponding to the first component (starting time, Ts1; ending time, Te1; starting frequency, Fs1; ending frequency, Fe1; shock speed, Vs1 and whether this starts during the flare impulsive phase, IP1) are given in columns 2–7. The shock speed is based on the 1× Newkirk coronal density model (Newkirk, 1961). Similarly, the data for the second component are given in columns 8–13. In column 14 (labeled as Remark), the possibility for the presence of multiple impulsive phases and/or multiple mass ejections are given.

Robinson and Sheridan (1982) suggested that there may be some relationships between different bands in a multiple type II event. When we looked into the relationship between the two components, we found weak correlations between the properties of the two components as shown in Figure 5. While the starting

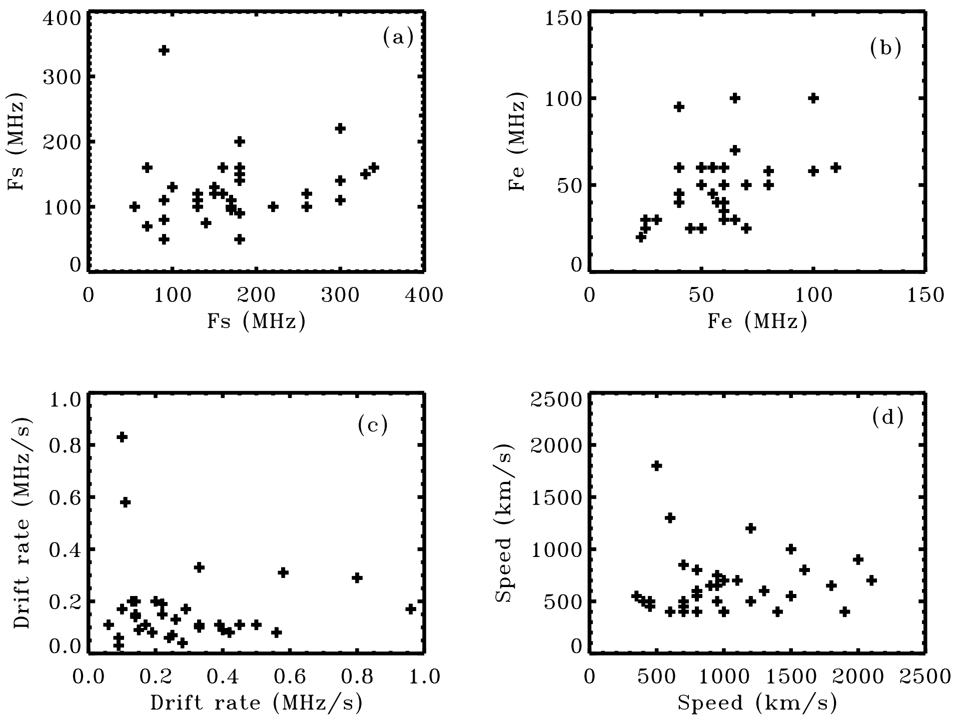

Figure 5. Comparison of the properties of first (along x-axis) and second (along y-axis) components (a) starting frequency, (b) ending frequency, (c) drift rate, (d) shock speed.

TABLE II

First and second components of multiple type II events.

Date	Ts1 (UT)	Te1 (UT)	Fs1 (MHz)	Fe1 (MHz)	Vs1 (km s^{-1})	IP1	Ts2 (UT)	Te2 (UT)	Fs2 (MHz)	Fe2 (MHz)	Vs2 (km s^{-1})	IP2	Remark
971103	04:37	04:50	260	55	700	Yes	04:50	04:57	90	58	500	–	
971104	05:58	06:07	230	30	1200	Yes	06:08	06:17	75	25	1200	–	
980125	21:35	21:55	90	40	350	Yes	21:56	22:38	60	35	550	–	
980423	05:40	05:43	140	45	1900	Yes	05:43	05:56	120	60	400	Yes	
980508	02:00	02:10	260	65	600	Yes	02:10	02:16	160	50	1300	–	
980509	03:26	03:29	150	50	1500	Yes	03:31	03:42	150	40	1000	Yes	*a*
980530	22:48	22:56	340	60	700	Yes	22:51	23:06	260	60	400	Yes	
980819	21:45	21:49	330	40	1200	Yes	21:53	21:58	100	45	600	–	
980824	22:02	22:18	140	18	1300	Yes	22:10	22:20	130	40	600	Yes	
980909	05:00	05:03	70	40	800	–	05:01	05:18	160	45	400	–	
980923	06:57	07:05	170	50	700	Yes	07:04	07:22	100	25	850	Yes	*a*
981124	02:17	02:22	150	60	1000	Yes	02:24	02:31	90	50	400	–	
981127	07:30	07:45	130	55	500	Yes	07:41	07:42	110	60	1800	Yes	*a*, *b*
981223	06:11	06:21	55	25	950	Yes	06:21	06:32	100	30	750	Yes	
990403	23:07	23:17	180	40	400	Yes	23:38	23:45	180	50	500	–	*b*
990526	02:35	02:44	160	50	650	–	02:44	02:49	120	60	–	–	
990611	00:39	00:49	250	50	950	Yes	00:49	01:00	130	40	500	Yes	
990711	00:14	00:19	170	70	800	Yes	00:20	00:28	100	50	600	–	
990802	21:29	21:40	220	60	700	–	21:39	21:58	100	30	450	–	
991116	05:07	05:20	90	23	950	Yes	05:16	05:31	50	20	650	–	
991228	00:46	00:55	300	55	800	Yes	00:56	01:06	110	45	550	–	

(*Continued on next page*)

TABLE II
(*Continued*)

Date	Ts1 (UT)	Te1 (UT)	Fs1 (MHz)	Fe1 (MHz)	Vs1 ($km\,s^{-1}$)	IP1	Ts2 (UT)	Te2 (UT)	Fs2 (MHz)	Fe2 (MHz)	Vs2 ($km\,s^{-1}$)	IP2	Remark
000212	04:03	04:12	180	60	800	Yes	04:12	04:19	140	60	800	–	*a*
000217	20:25	02:40	180	26	800	Yes	20:38	20:49	150	40	550	–	
000327	06:46	06:54	180	40	1400	Yes	06:49	07:06	130	45	400	Yes	
001009	23:37	23:45	70	25	1000	Yes	23:43	23:55	70	25	700	Yes	*a*, *b*
001124	05:02	05:11	180	30	1100	Yes	05:19	05:28	50	30	700	–	
001125	01:07	01:16	150	18	2000	Yes	01:14	01:20	90	30	900	Yes	
010120	21:12	21:22	250	20	1600	Yes	21:18	21:26	180	55	800	Yes	
010520	06:04	06:06	180	65	2100	–	06:05	06:24	340	25	700	–	
010611	05:54	05:57	90	70	–	–	06:00	06:09	100	30	800	–	
011019	01:00	01:12	180	57	500	Yes	01:01	01:03	220	70	1800	Yes	*b*
011108	07:04	07:10	300	65	1000	Yes	07:07	07:26	140	57	400	–	
020409	00:42	00:44	400	220	900	Yes	00:44	00:51	240	80	450	–	
020412	04:58	05:01	150	110	600	Yes	05:05	05:09	130	95	400	Yes	*a*
021110	03:16	03:23	100	40	800	Yes	03:20	03:34	160	40	600	Yes	
030123	04:33	04:45	160	57	450	Yes	04:47	05:03	140	35	450	–	*a*, *b*
030423	01:01	01:06	300	60	1500	Yes	01:06	01:15	130	50	550	Yes	
030527	23:02	23:10	180	100	900	Yes	23:11	23:16	200	100	650	–	*b*

Note. Please see the text for more details regarding the labels in the first row.
a – There may be multiple impulsive phases of flares.
b – There may be multiple mass ejections.

and ending frequencies show weak correlations (Figure 5a and b), it is not seen between their drift rates or their shock speeds (Figure 5c and d). This may be attributed to either different density gradients at different shock segments or involvement of different shocks. Results from the Student's t-test show that all correlations in Figure 5 have significantly different means except the ending frequency (Figure 5b). In this test, p-value of less than 0.05 means that the two samples have significantly different means. But, the p-value is around 0.121 in the case of ending frequency.

Results from the recent literatures (Svestka and Svestkova, 1974; Klassen *et al.*, 1999; Vrsnak *et al.*, 1995; Vrsnak, 2001; Classen and Aurass, 2002; Mann *et al.*, 2003; Shanmugaraju *et al.*, 2003a) show that the back-extrapolation of type II emission (usually) marks the impulsive phase. Regarding this, we compared the timing details: flare peak time, and the starting times of first and second components. In agreement of the aforementioned results, in all except five events, the first component occurred in the impulsive phase (in these five cases, the time delay is only less than 5 min). However, in 22 out of 38 events, the second components started after flare peak time. That is, they did not start within the flare impulsive phase. Significantly, the second component started 10 min after flare peak time in 10 cases. Hence, it is essential to identify the sources of these second components as discussed in the following section.

4. Discussion

In the present paper, we have compiled a large sample of multiple type IIs. As seen in Figure 4, the properties of the individual components in a multiple type II agree with those of the general type IIs. The time delay between the two components in a single multiple type II event ranges from 0 to 20 min. It may be noted that the flares and CMEs start closely in time within a time interval of a few minutes (Neupert *et al.*, 2001; Zhang *et al.*, 2001). More recently, it has been found that the CME acceleration phase is synchronized with the impulsive phase of the flare (Shanmugaraju *et al.*, 2003b; Vrsnak *et al.*, 2004; Zhang *et al.*, 2004).

In general, the starting frequency, drift rate and the shock speed of the first component are higher than that of the second component. However, this is not so in a few cases. This may be attributed to the shape and propagation of the shocks through different coronal structures.

As given in Table I, almost all the multiple type II events are associated with flares and CMEs. This is similar to that of Robinson and Sheridan (1982). In the present study, the physical characteristics of the flares and CMEs (duration and strength of the flares, speed and width of the CMEs) are investigated using a large data set and found that the energy released in a multiple type II event seems to be high. More specifically, 75% of the flares are greater than M1 class, and 50% of the CMEs have their widths larger than 200°.

Are these multiple type IIs generated by a single shock traveling through different coronal structures? Or, are they generated by multiple shocks from distinct drivers? In this context, it will be more interesting to discuss further as follows. The relatively higher values of starting frequency, drift rate, and shock speed of the first component may imply that they are due to flare blast waves (for example, see, Wagner and MacQueen, 1983; Nelson and Melrose, 1985; Vrsnak *et al.*, 1995; Klassen *et al.*, 1998; Gopalswamy, 2000). That is, type II shocks formed by flares at comparatively low coronal height where the electron density is high, hence, so is the higher plasma frequency. The plasma frequency (f_p in MHz) is related to electron density (n_e in cm^{-3}) as $f_p = 0.009\, {n_e}^{1/2}$. On the other hand, the CME-driven shocks are formed in the upper corona where the electron density is low and so the lower plasma frequency. Recently, Reiner *et al.* (2003) presented a contradictory argument that the CME-driven shock that produces type II emission can sometimes form very low in the corona.

As proposed by Robinson and Sheridan (1982), the multiple type IIs might be produced by a single shock traveling through different coronal structures (also see Knock and Cairns, 2005). While some theoretical models explain the generation of multiple type IIs either by a single flare (Odstrcil and Karlicky, 2000) or by a coronal mass ejection (Magara *et al.*, 2001), such multiple type IIs could be associated with complex flares showing several impulsive phases. First, we examined the possibilities of multiple impulsive phases for the events presented in Table I. For example, two such events are given in Figure 6, which shows clearly the presence of multiple impulsive phases. Particularly for the event on January 23, 2003, the flare peak times (04:34 and 04:48 UT) of two X-ray flares nearly correspond to the starting times of two type II bursts. It may imply the possibility that two flare blast wave shocks (flare–flare) are responsible for the multiple type II event. According to the RHESSI data (http://www.hedc.ethz.ch/hedc/), both flares occurred in the same active region. So we can say that the flares are similar to homologous events. It may be emphasized that both type IIs in Figure 1 are very similar ("homologous" type II bursts). This indicates that two successive homologous flare events generated two successive homologous type II bursts. However, corresponding to these two flares on January 23, 2003, there were also two coronal mass ejections seen in LASCO (05:30 and 05:54 UT). But, two CMEs seen in LASCO C2 images have quite different position angle and angle width. So we can not say that they are homologous events.

In a few other cases, as mentioned in Table II, there may be multiple impulsive phases, but they are not so clear as shown in Figure 6. As described in the previous section, almost all the first components started during the impulsive phase of the flares. They may be assumed to be generated by flare blast wave shocks. In 22 out of 38 events, the second component started after the flare impulsive phase. It may be speculated that these components were caused by CMEs (CME front or CME flank). In addition, even though there are some weak relations found between the properties of two components (as seen in Figure 5 in Section 3.2), the weak

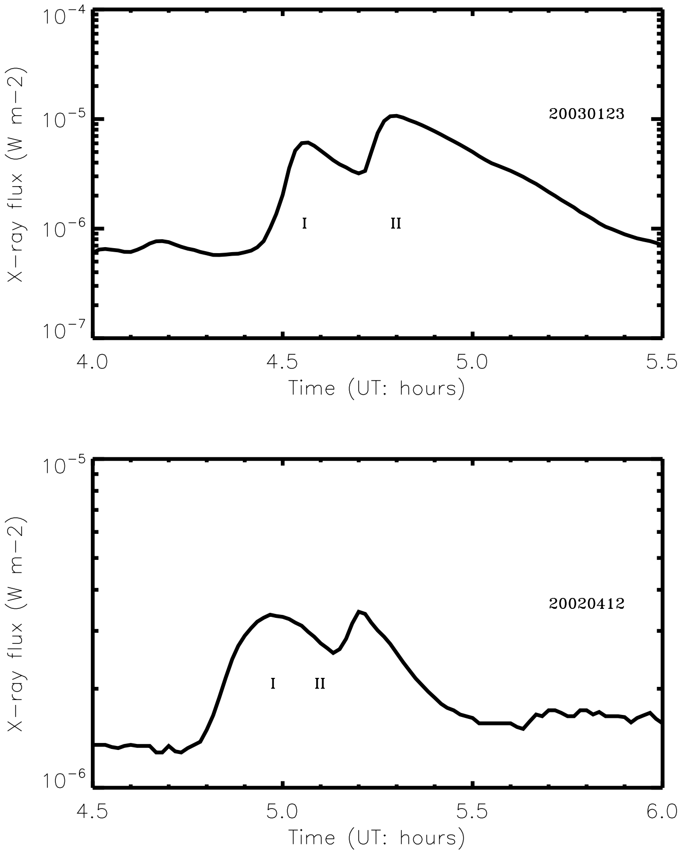

Figure 6. Multiple X-ray peaks observed for two different events. I and II represent the starting times of first and second type IIs, respectively.

correlations may also be ascribed due to the involvement of two shocks generated by distinct drivers. As already mentioned in Section 1, evidence for more than one coronal shock or more than one coronal shock source has been provided recently in the literature.

Furthermore, some of the metric type IIs may be explained by only CMEs (for example, Reiner *et al.*, 2003; Vourlidas *et al.*, 2003; Mancuso and Raymond, 2004; Ciaravella *et al.*, 2005; Cliver *et al.*, 2004) rather than flares. In addition, Vrsnak, Magdalenic, and Aurass (2001) suggested that nearly 10% of metric type IIs might be caused by CMEs accidentally associated with flares. In the present study, the mean speed of CMEs associated with multiple type II bursts (875 km s^{-1}) is slightly higher than the mean speed ($\sim$700 km s^{-1}) in an overall sample of CMEs associated with metric type II bursts (Lara *et al.*, 2003; Shanmugaraju *et al.*, 2003c). More specifically, the fast CMEs may also produce shocks in the corona. Also, when the width of the CMEs is large, the shock generated by the CMEs may be big

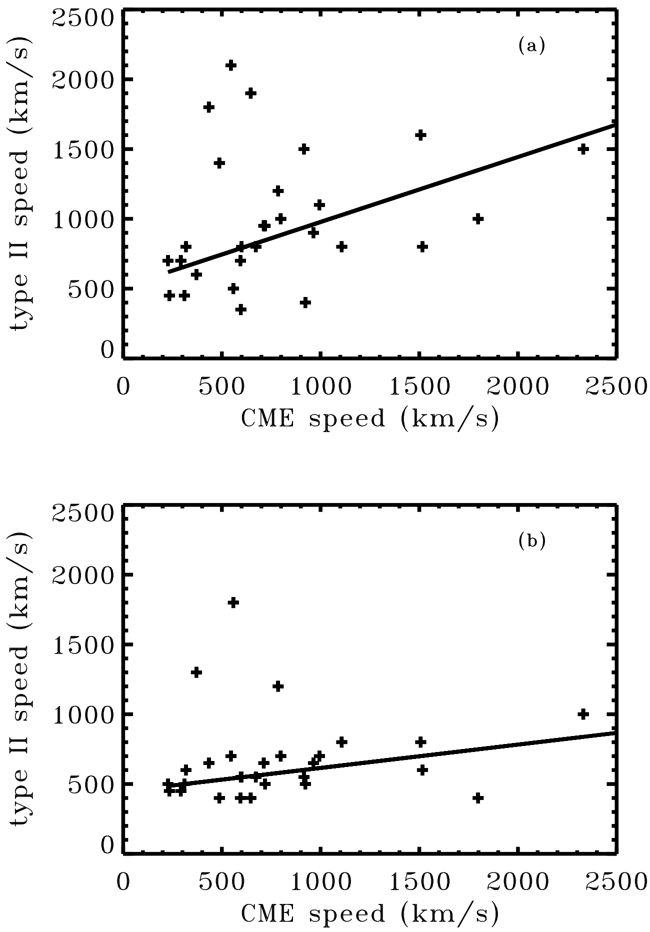

Figure 7. Correlation between (a) first component speed and CME speed, (b) second component speed and CME speed.

enough to sweep through different coronal structures (Sheeley, Hakala, and Wang, 2000). As mentioned earlier, 50% of the CMEs in the present study have widths larger than 200°. Also in the present study, a weak correlation is found between the CME and type II speeds (Figure 2). The large scattered distributions in Figure 2 may be attributed to projection effect, coronal density model, and non-CME origin, etc. Figure 7 shows the relationships separately between CME speeds and the speeds of the first and the second components. There seems to be better correlations (correlation coefficient ∼0.8) than the case of Figure 2 when we neglect the three isolated cases in the top of each figure (Figure 7a and b). While the slope in Figure 7b is nearly 0.5, it is nearly equal to one in Figure 7a. Note that the CME speed in Figure 7 corresponds to the speed of the CME front. This large difference in the slope may be explained by a third possibility that CME front and CME flank are responsible for the multiple type IIs, since the speed of the CME flank is less than that of the CME front. This fact has been demonstrated both theoretically (Dryer *et al.*, 1979; Vourlidas *et al.*, 2003) and observationally (Sheeley, Hakala, and Wang, 2000).

A group of fast CMEs, in Figures 2 and 7b, has slow type IIs most likely are not being driven by CMEs (Vrsnak and Lulic, 2000). Similarly, the three "isolated" fast type II bursts associated with slow CMEs (in Figure 7a and b) are also more likely to be generated by flares. This is also evident from the type II speed–flare importance graph (Figure 2b) that these high-speed type IIs alone will increase the correlation.

Summarizing all the earlier discussion, different components in a multiple type II event might be assumed to be generated by (a) a single shock traveling through different coronal structures or (b) a combination of shocks (i) flare–flare, (ii) flare–CME front or CME flank, and (iii) CME front–CME flank. However, in case (b), because almost all the events in our study are associated with both flares and CMEs, it may be suggested that the possibility (ii) can be accounted for multiple type IIs.

5. Conclusion

We report on the detailed analysis of a set of 38 multiple type II radio bursts observed by Culgoora radio spectrograph and reported in Solar Geophysical Data from January 1997 to July 2003. These events were selected on the basis of the following criteria: (i) more than one type II bursts were reported within a 30 min interval, (ii) both fundamental and harmonic traces were identified for each of them. The X-ray flares and CMEs corresponding to these events are identified using GOES, Yohkoh and SOHO data. From the analysis of these events, we found that (i) two type IIs with fundamental and harmonic are reported in many cases, and the time interval between the two type IIs is within 15 min, (ii) the mean values of starting frequency, drift rate, and shock speed of the first type II are significantly higher than those of the second type II, (iii) more than 90% of these events are associated with both X-ray flares and CMEs, (iv) nearly 75% of the flares are greater than M1 X-ray class and 50% of CMEs have widths more than 200° or they are halo CMEs, (v) while there is a weak relationship between the starting frequency of the two type IIs and ending frequency of the two type IIs, it is not seen in the case of shock speeds. Moreover, in 22 out of 38 cases, the second component started after the flare impulsive phase. It may be suggested that the probability of observing the multiple type IIs is higher when the strength of the flares is high, and the width of the CMEs is large. The results are also discussed with a focus on the various possibilities on the origin of multiple type IIs.

As a result, different components in a multiple type II event might be assumed to be generated by a single shock traveling through different coronal structures.

However, considering the results that there are no events which are only associated with multiple flares or only associated with multiple mass ejections and almost all the events are associated with both flares and CMEs, it may be suggested that the flares and CMEs (front or flank) both might be the sources of multiple type IIs.

Acknowledgements

The authors are grateful to the referee Dr. B. Vrsnak for his very helpful suggestions. We kindly acknowledge the various online catalogs (CMEs, flares, type IIs) and to their open data policy. We wish to thank Dr. Nigel Prestage for providing the type II radio bursts data. Y.-J. Moon and K.-S. Cho have been supported by the MOST grants (M1-0104-00-0059 and M1-0407-00-0001) of the Korean government. M.D. has been partially supported by a U.S. DoD/USAF/UPOS project (via the University of Alaska at Fairbanks, Geophysical Institute) and by a NASA/LWS contract to Exploration Physics International, Inc. The CME catalog we have used is generated and maintained by the Center for Solar Physics and Space Weather, The Catholic University of America in cooperation with the Naval Research Laboratory and NASA. *SOHO* is a project of international cooperation between ESA and NASA. Part of this work was conducted during A.S.'s visit to Korea Astronomy and Space Science Institute (KASI), Korea.

References

Ciaravella, A., Raymond, J. C., Kahler, S. W., Vourlidas, A., and Li, J.: 2005, *Astrophys. J.* **621**, 1121.

Classen, H. T. and Aurass, H.: 2002, *Astron. Astrophys.* **384**, 1098.

Cliver, E. W., Nitta, N. V., Thompson, B. J., and Zhang, J.: 2004, *Solar Phys.* **225**, 105.

Dryer, M., *et al.*: 1979, *Astrophys. J.* **227**, 1059.

Gergely, T. E., Kundu, M. R., Wu, S. T., Dryer, M., Smith, Z. K., and Stewart, R. T.: 1984, *Adv. Space. Res.* **4**(7), 283.

Gopalswamy, N.: 2000, in R. G. Stone, *et al.* (eds.), *AGU Monograph* 119, American Geophysical Union, Washington, DC, p. 123.

Kaiser, M. L., Reiner, M. J., Howard, R. A., Gopalswamy, N., St. Cyr, O. C., Thompson, B. J., and Bourgeret, J. L.: 1998, *Geophys. Res. Lett.* **25**, 2501.

Klassen, A., Aurass, H., Klein, K.-L., Hofmann, A., and Mann, G.: 1999, *Astron. Astrophys.* **343**, 287.

Klassen, A., Karlicky, M., Aurass, H., and Jiricka, K.: 1999, *Solar Phys.* **188**, 141.

Knock, S. A. and Cairns, I. H.: 2005, *J. Geophys. Res.* **110**(A1), doi: 10.1029/2004JA010452.

Lara, A., Gopalswamy, N., Nunes, S., Muoz, G., and Yashiro, S.: 2003, *Geophys. Res. Letters* **30**(12), 8016, doi: 10.1029/2002GL016481.

Leblanc, Y., Dulk, G. A., Vourlidas, A., and Bougeret, J. L.: 2001, *J. Geophys. Res.* **106**(A11), 25301.

Magara, T., Chen, P., Shibata, K., and Yokoyama, T.: 2001, *Astrophys. J.* **538**, L175.

Mancuso, S. and Raymond, J. C.: 2004, *Astron. Astrophys.* **413**, 363.

Mann, G., Klassen, A., Aurass, H., and Classen, H.-T.: 2003, *Astron. Astrophys.* **400**, 329.

Maxwell, A. and Dryer, M.: 1982, *Space Sci. Rev.* **32**, 11.
Moon, Y.-J., Choe, G. S., Wang, H., Park, Y. D., Gopalswamy, N., Yang, G., and Yashiro, S.: 2002, *Astrophys. J.* **581**, 694.
Nelson, G. J. and Melrose, D. B.: 1985, in D. J. McLean and N. R. Labrum (eds.), *Solar Radiophysics*, Cambridge University Press, Cambridge, p. 350.
Neupert, W. M., Thompson, B. J., Gurman, J. B., and Plunkett, S. P.: 2001, *J. Geophys. Res.* **106**, 25215.
Newkirk, G. A.: 1961, *Astrophys. J.* **133**, 983.
Odstrcil, D. and Karlicky, M.: 2000, *Astron. Astrophys.* **359**, 766.
Reiner M. J., Kaiser, M. L., Gopalswamy, N., Aurass, H., Mann, G., Vourlidas, A., and Maksimovic, M.: 2001, *J. Geophys. Res.* **106**(A11), 25279.
Reiner M. J., Vourlidas, A., St. Cyr, O. C., Burkepile, J. T., Howard, R. A., Kaiser, K. L., Prestage, N. P., and Bougeret, J.-L.: 2003, *Astrophys. J.* **590**, 533.
Robinson, R. D.: 1985, *Solar Phys.* **95**, 343.
Robinson, R. D. and Sheridan, K. V.: 1982, *Proc. Astron. Soc. Aust.* **4**, 392.
Shanmugaraju, A., Moon, Y.-J., Dryer, M., and Umapathy, S.: 2003a, *Solar Phys.* **215**, 161.
Shanmugaraju, A., Moon, Y.-J., Dryer, M., and Umapathy, S.: 2003b, *Solar Phys.* **215**, 184.
Shanmugaraju, A., Moon, Y.-J., Dryer, M., and Umapathy, S.: 2003c, *Solar Phys.* **217**, 301.
Sheeley, N. R., Jr., Hakala, W. N., and Wang, Y.-M.: 2000, *J. Geophys. Res.* **105**(A3), 5081.
Svestka, Z. and Fritzova-Svestkova, L.: 1974, *Solar Phys.* **36**, 417.
Vourlidas, A., Wu, S. T., Wang, A. H., Subramanian, P., and Howard, R. A.: 2003, *Astrophys. J.* **598**, 1392.
Vrsnak, B., Ruzdjak, V., Zlobec, P., and Aurass, H.: 1995, *Solar Phys.* **158**, 331.
Vrsnak, B. and Lulic, S.: 2000, *Solar Physics* **196**, 157.
Vrsnak, B.: 2001, *J. Geophys. Res.* **106**(A11), 25291.
Vrsnak, B., Magdalenic, J., and Aurass, H.: 2001, *Solar Phys.* **202**, 319.
Vrsnak, B., *et al.*: 2001, *Astron. Astrophys.* **377**, 321.
Wagner, W. J. and MacQueen, R. M.: 1983, *Astron. Astrophys.* **120**, 136.
Zhang, J., Dere, K. P., Howard, R. A., Kundu, M. R., and White, S. M.: 2001, *Astrophys. J.* **559**, 452.
Zhang, J., Dere, K. P., Howard, R. A., and Vourlidas, A.: 2004, *Astrophys. J.* **604**, 420.